

## $\beta$ -Hairpins Generated from Hybrid Peptide Sequences Containing both $\alpha$ - and $\beta$ -Amino Acids

by Hosahudya N. Gopi<sup>a</sup>), Rituparna S. Roy<sup>a</sup>), Srinivasa R. Raghothama<sup>b</sup>), Isabella L. Karle<sup>c</sup>), and Padmanabhan Balaram<sup>\*a</sup>)

<sup>a</sup>) Molecular Biophysics Unit, Indian Institute of Science, Bangalore-560012, India  
(phone: (080)-3092337; fax: (080)-3600683, 3600535; e-mail: pb@mbu.iisc.ernet.in)

<sup>b</sup>) Sophisticated Instruments Facility, Indian Institute of Science, Bangalore-560012, India

<sup>c</sup>) Laboratory for the Structure of Matter, Naval Research Laboratory, Washington, D.C. 20375-5341

Dedicated to Professor *Dieter Seebach* on the occasion of his 65th birthday

The incorporation of the  $\beta$ -amino acid residues into specific positions in the strands and  $\beta$ -turn segments of peptide hairpins is being systematically explored. The presence of an additional torsion variable about the  $C(\alpha)-C(\beta)$  bond ( $\theta$ ) enhances the conformational repertoire in  $\beta$ -residues. The conformational analysis of three designed peptide hairpins composed of  $\alpha/\beta$ -hybrid segments is described: Boc-Leu-Val-Val-<sup>D</sup>Pro- $\beta$ Phe-Leu-Val-Val-OMe (**1**), Boc-Leu-Val- $\beta$ Val-<sup>D</sup>Pro-Gly- $\beta$ Leu-Val-Val-OMe (**2**), and Boc-Leu-Val- $\beta$ Phe-Val-<sup>D</sup>Pro-Gly-Leu- $\beta$ Phe-Val-Val-OMe (**3**). 500-MHz <sup>1</sup>H-NMR Analysis supports a preponderance of  $\beta$ -hairpin conformation in solution for all three peptides, with critical cross-strand NOEs providing evidence for the proposed structures. The crystal structure of peptide **2** reveals a  $\beta$ -hairpin conformation with two  $\beta$ -residues occupying facing, non-H-bonded positions in antiparallel  $\beta$ -strands. Notably,  $\beta$ Val(3) adopts a *gauche* conformation about the  $C(\alpha)-C(\beta)$  bond ( $\theta = +65^\circ$ ) without disturbing cross-strand H-bonding. The crystal structure of **2**, together with previously published crystal structures of peptides **3** and Boc- $\beta$ Phe- $\beta$ Phe-<sup>D</sup>Pro-Gly- $\beta$ Phe- $\beta$ Phe-OMe, provide an opportunity to visualize the packing of peptide sheets with local 'polar segments' formed as a consequence of reversal peptide-bond orientation. The available structural evidence for hairpins suggests that  $\beta$ -residues can be accommodated into nucleating turn segments and into both the H-bonding and non-H-bonding positions on the strands.

**Introduction.** – The stereochemistry of polypeptide chains composed of  $\alpha$ -amino acid residues has been extensively investigated since *Pauling's* remarkable insights led to the elucidation of the  $\alpha$ -helix and  $\beta$ -sheet structures [1][2]. The recognition by *Ramachandran* and co-workers that stereochemically allowed conformations of polypeptide chains may be conveniently analyzed in torsion angle ( $\theta, \psi$ ) space, with each residue exhibiting two degrees of freedom, was a major advance in the development of polypeptide stereochemistry [3][4]. The focus of much work over the past several decades has been on polypeptides composed of  $\alpha$ -amino acids, with natural proteins being pre-eminent examples [5]. Considerable attention has also been paid to the use of stereochemically constrained amino acids and templates in the design of folded polypeptides, with  $\theta, \psi$ -restrictions being imposed by backbone modifications like substitution, chirality reversal, and cyclization [6–8]. In principle, the introduction of additional degrees of torsional freedom into the polypeptide backbone by insertion of methylene groups must expand the conformational repertoire. Early work on polyamides related to the nylons did indeed suggest the possibility of novel folded structures for poly- $\beta$ -amino acids, hitherto unknown in the area of poly- $\alpha$ -amino acids

[9][10]. The structural characterization of the conformations exhibited by peptides composed of  $\beta$ -amino acids received a major thrust when *Seebach* and co-workers initiated a comprehensive and incisive analysis of the stereochemistry of  $\beta$ -peptide chains [11–15]. The expanded range of novel polypeptide structures that could be achieved in poly- $\beta$ -peptides was vividly illustrated in the crystallographic characterization of the 12-helix and 14-helix, in the structures of oligomers of *trans*-2-aminocyclopentanecarboxylic acid (ACPC) and *trans*-2-aminocyclohexanecarboxylic acid (ACHC), respectively, by *Gellman* and co-workers [16–19]. The major lessons that have been learnt, thus far, from the growing body of work on  $\beta$ -peptides are: *i*) Novel H-bonding patterns, with reversal of directionality of donors and acceptors and reversal of the sense of helix twist, may be obtained in  $\beta$ -peptide helices. *ii*) ‘Polar’  $\beta$ -sheets are formed by  $\beta$ -peptides with a net dipole moment perpendicular to the strand direction in contrast to sheets formed by  $\alpha$ -peptides.

As part of a program to develop the use of  $\alpha/\beta$ - and  $\alpha/\omega$ -hybrid sequences in peptide design, we have been exploring the consequences of incorporating  $\beta$ -residues and higher homologues as guests into host  $\alpha$ -amino acid sequences [20]. This approach is of relevance in the generation of biologically active peptide analogs exhibiting resistance to proteolysis, with susceptible cleavage sites modified by insertion of  $\beta$ -residues [21][22].

The discussion of the conformational properties of  $\beta$ -residues is based on three degrees of conformational freedom:  $\phi(N-C(\beta))$ ,  $\theta(C(\beta)-C(\alpha))$ , and  $\psi(C(\alpha)-CO)$ . The  $\phi, \theta, \psi$ -nomenclature [23][24] permits labeling of torsion angles sequentially from the N-terminus of the peptide chain, allowing a direct comparison with the vast body of conformational information on  $\alpha$ -peptides. *Fig. 1* shows a distribution of available  $\beta$ -residue conformations in a 3-dimensional  $\phi, \theta, \psi$ -diagram. In general,  $\theta$  values of  $\pm 60^\circ$  and  $180^\circ$  are observed. The *gauche* conformers are generally obtained in folded helical and turn structures while the *trans* form is seen in cases of extended strands. In cyclic  $\beta$ -amino acids, like ACPC,  $\theta$  values as large as  $90^\circ$  are observed.

In this report, we specifically address the issue of inserting  $\beta$ -residues at the turn and strand positions of peptide hairpins. *Fig. 2, a* schematically illustrates the hairpin structure. In principle, four distinct sites for  $\beta$ -residue substitution may be considered. These are the  $i+1$  and  $i+2$  positions of the  $\beta$ -turn and the H-bonding and non-H-bonding positions on the pair of antiparallel strands. Peptide hairpins have been successfully nucleated with the  $^D$ Pro-Gly  $\beta$ -turn motif (*Fig. 2, b*). In the area of  $\beta$ -peptides, two potential hairpin-nucleating motifs have been reported in the literature. *Seebach et al.* have suggested the  $C_{10}$  H-bonded structure (*Fig. 2, c*) as a hairpin nucleator [25]. An isolated  $C_{10}$ -turn structure has been crystallographically characterized in a model tripeptide [26]. *Gellman* and co-workers have advanced the use of heterochiral dinipicotic acid (1-(3-piperidinylcarbonyl)piperidine-3-carboxylic acid) segments, which form a  $C_{12}$  H-bonded turn facilitating antiparallel-hairpin formation [27]. We have previously established the structures of crystalline peptide hairpins that contain  $\beta$ -amino acids in the strand positions. In this report, we describe the structural characterization of three  $\alpha, \beta$ -hybrid peptides, which contain  $\beta$ -residues at chosen positions: Boc-Leu-Val-Val- $^D$ Pro- $\beta$ Phe-Leu-Val-Val-OMe<sup>1)</sup> (**1**), Boc-Leu-Val- $\beta$ Val-

<sup>1)</sup>  $\beta^3$ -(*S*)-Homophenylalanine is abbreviated as  $\beta$ Phe for simplicity.

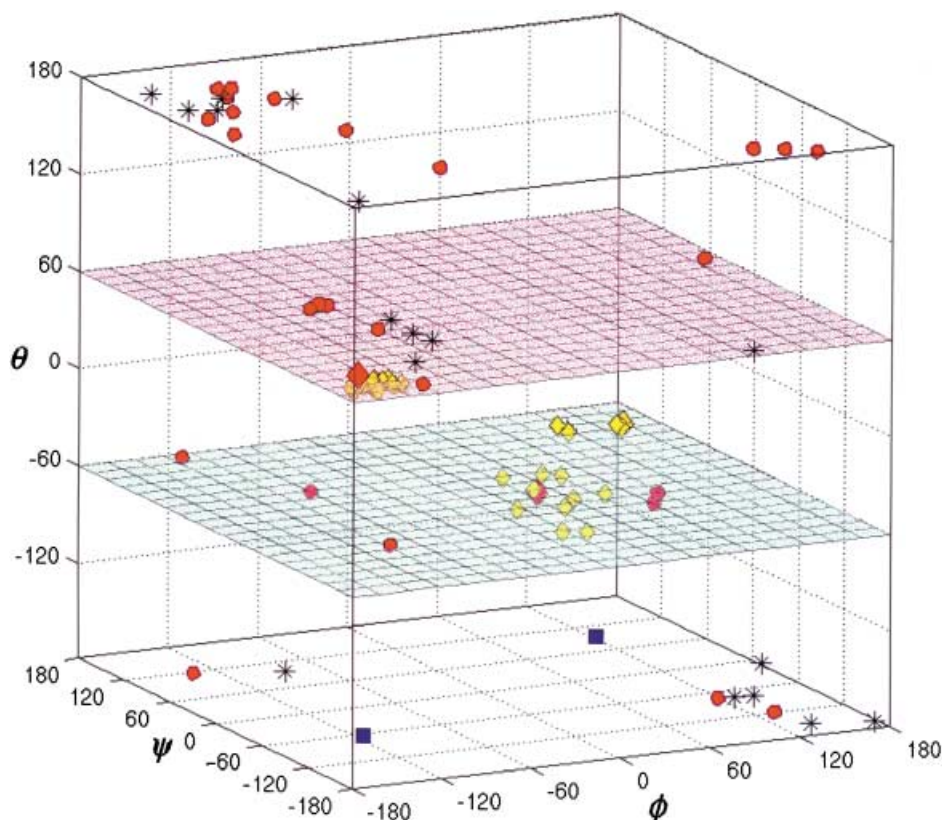


Fig. 1. Distribution of crystallographically observed  $\beta$ -residues conformation in  $\phi, \theta, \psi$ -conformational space. The shaded planes highlight *gauche* conformations of  $\beta$ -residues about the  $C(\alpha)-C(\beta)$  bond. \*: Observation for the chiral acyclic  $\beta$ -amino acid,  $\beta$ -glycine (referred to in the early literature as  $\beta$ -alanine, correctly designated as  $\beta$ -glycine); in the case of achiral peptides crystallizing in centric space groups, one sign of the dihedral angles was arbitrarily taken.  $\circ$ : Chiral acyclic  $\beta$ -amino acids.  $\diamond$  (yellow): Chiral cyclic  $\beta$ -amino acids.  $\square$ : Nipicotic acid (= piperidine-3-carboxylic acid) (this is shown separately because the constraints of cyclization restrict both  $\phi$  and  $\theta$  values [27]).  $\diamond$  (red): Idealized 14- and 12-helix structures.

$^{\text{D}}\text{Pro-Gly-}\beta\text{Leu-Val-Val-OMe}^2)^3$  (**2**), and  $\text{Boc-Leu-Val-}\beta\text{Phe-Val-}^{\text{D}}\text{Pro-Gly-Leu-}\beta\text{Phe-Val-Val-OMe}$  (**3**). The anticipated hairpin forms are illustrated in *Fig. 3*. The results presented here are compared with those for two previously studied peptides:  $\text{Boc-Leu-Val-Val-}^{\text{D}}\text{Pro-Gly-Leu-Val-Val-OMe}$  (**4**) and  $\text{Boc-}\beta\text{Phe-}\beta\text{Phe-}^{\text{D}}\text{Pro-Gly-}\beta\text{Phe-}\beta\text{Phe-OMe}$  (**5**).

Peptide **4** is the canonical  $\alpha$ -peptide hairpin, whose conformation has been established in both solution [28][29] and in the solid state [30]. Peptide **5** has been crystallographically characterized [31].

<sup>2)</sup>  $\beta^3$ -(*R*)-Homovaline ( $\beta\text{Val}$ ) was generated from (*S*)-valine. Note the formal change of configuration assignment upon homologation [14].

<sup>3)</sup>  $\beta^3$ -(*S*)-Homoleucine ( $\beta\text{Leu}$ ) was generated from (*S*)-leucine.

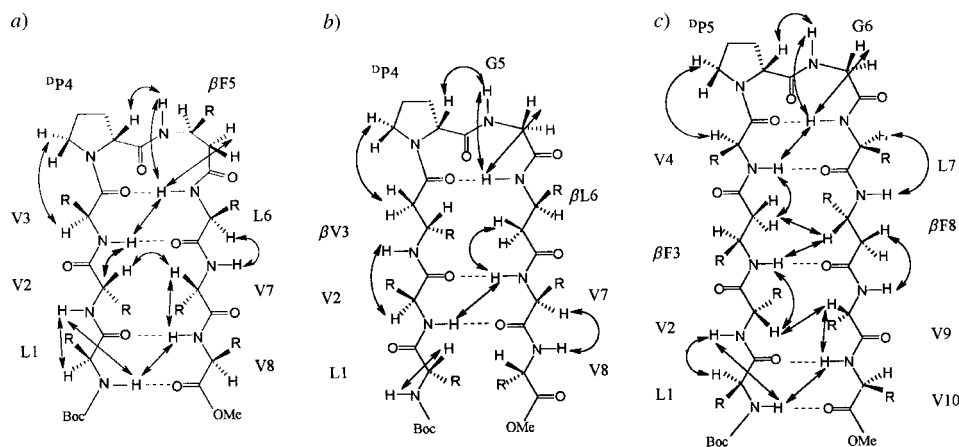
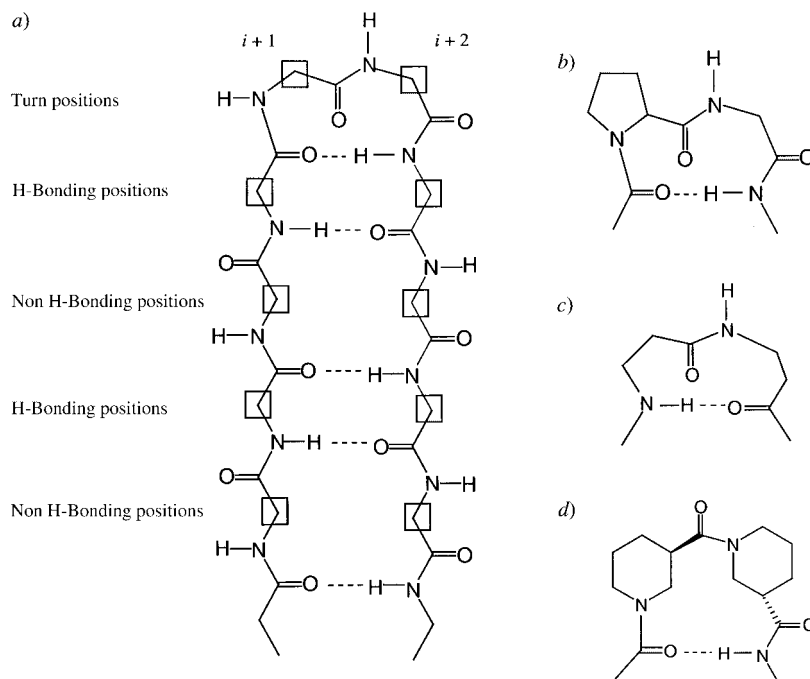


Fig. 3. Schematic representation of proposed  $\beta$ -hairpins of a) peptide 1, b) peptide 2, and c) peptide 3. The observed NOEs, indicated by double edged arrows, determine the  $\beta$ -hairpin conformations.

**Results and Discussion.** – *NMR Analysis of Peptide 1.* Sequence-specific assignments were achieved by means of a combination of TOCSY and ROESY experiments. The chemical shifts are summarized in *Table 1*. *Fig. 4* shows partial sections of the ROESY spectrum of **1**. It is evident that strong sequential, inter-residue  $d_{\alpha\text{N}}$ -connectivities were observed, while  $d_{\text{NN}}$ -sequential connectivities are weak or absent. This suggests that extended conformations are favored for residues 1–3 and 6–8. A weak  $d_{\text{NN}}$ -connectivity is indeed observed between N–H( $\beta$ Phe(5)) and N–H(Leu(6)) protons supporting chain reversal. Most importantly, the cross-strand NOEs  $d_{\text{NN}}$  (1/8) and  $d_{\text{NN}}$  (3/6) are observed (*Fig. 4*), which are characteristic of a registered pair of antiparallel strands (*Fig. 3*). In addition, the  $d_{\alpha\alpha}$  (2/7) is also observed despite the limited chemical-shift dispersion of the resonances. The NMR data strongly support a major population of  $\beta$ -hairpin conformations in peptide **1**.

Table 1.  $^1\text{H-NMR}$  (500 MHz) Chemical Shifts ( $\delta$  in ppm) for Peptide **1** at 300 K in  $\text{CDCl}_3$

Residue	N–H	H–C( $\alpha$ )	H–C( $\beta$ )	Others
Leu(1)	5.68	4.15	1.65	1.55 (H–C( $\gamma$ )); 0.90 (2 Me( $\delta$ ))
Val(2)	6.63	4.78	1.94	0.6, 0.93 (2 Me( $\gamma$ ))
Val(3)	8.39	4.61	2.05	0.91 (2 Me( $\gamma$ ))
$^{\text{D}}$ Pro(4)		4.30	2.10	1.89, 1.98 ( $\text{CH}_2(\gamma)$ ); 3.53, 3.72 ( $\text{CH}_2(\delta)$ )
$\beta$ Phe(5)	6.49	2.50, 2.59	4.09	2.90, 2.95 ( $\text{CH}_2(\gamma)$ ); 7.10–7.26 (arom. H)
Leu(6)	7.43	4.65	1.81	1.62 (H–C( $\gamma$ )); 0.95 (2 Me( $\delta$ ))
Val(7)	6.94	4.69	2.02	0.98 (2 Me( $\gamma$ ))
Val(8)	8.09	4.59	2.18	0.94 (2 Me( $\gamma$ ))

*NMR Analysis of Peptide 2.* Peptide **2** contains  $\beta$ Val at position 3 and  $\beta$ Leu at position 6, which should occupy the facing H-bonding positions in the putative hairpin structure (*Fig. 3*). In  $\text{CDCl}_3$ , **2** yielded a poorly dispersed  $^1\text{H-NMR}$  spectrum. Further analyses were, therefore, carried out in  $\text{CD}_3\text{OD}$ . Resonances were readily assigned by means of a combination of TOCSY and ROESY experiments. The chemical shifts are summarized in *Table 2*. Relevant sections of the ROESY spectrum are illustrated in *Fig. 5*. A strong  $d_{\text{NN}}$  (5/6) connectivity confirms that Gly(5) adopts a local helical conformation, consistent with occupying a  $\beta$ -turn position. A cross-strand  $d_{\text{NN}}$  (2/7) NOE also supports the hairpin conformation shown in *Fig. 3*. Strong sequential inter-residue  $d_{\alpha\text{N}}$  connectivities are observed for Val(2)–Val(7) strand residues. The strong NOE between N–H(Val(7)) and H–C( $\alpha$ )( $\beta$ Leu(6)) protons provides further support for the proposed conformation. A  $d_{\alpha\text{N}}$  ( $i, i+2$ ) NOE is also observed between H–C( $\alpha$ )( $^{\text{D}}$ Pro) and N–H( $\beta$ Leu(6)) (*Fig. 5, a*), which is suggestive of a type-I' structure. The  $d_{\text{NN}}$  (1/2) NOE prominently seen in *Fig. 5, b* has been generally observed in peptide hairpins and is likely to be an indicator of fraying of strands at the termini.

*NMR Analysis of Peptide 3.* In this designed decapeptide hairpin, the two  $\beta$ Phe residues have been inserted into the sequence of the canonical  $\beta$ -hairpins **4**, such that they occupy facing non-H-bonding positions. Since well-dispersed NMR spectra of peptide **3** were obtained in  $\text{CD}_3\text{OD}$ , all subsequent analyses were carried out in this solvent. Peptide **3** also exhibits extremely good dispersion in  $\text{CDCl}_3$ . Resonance assignments were possible by means of a combination of TOCSY and ROESY

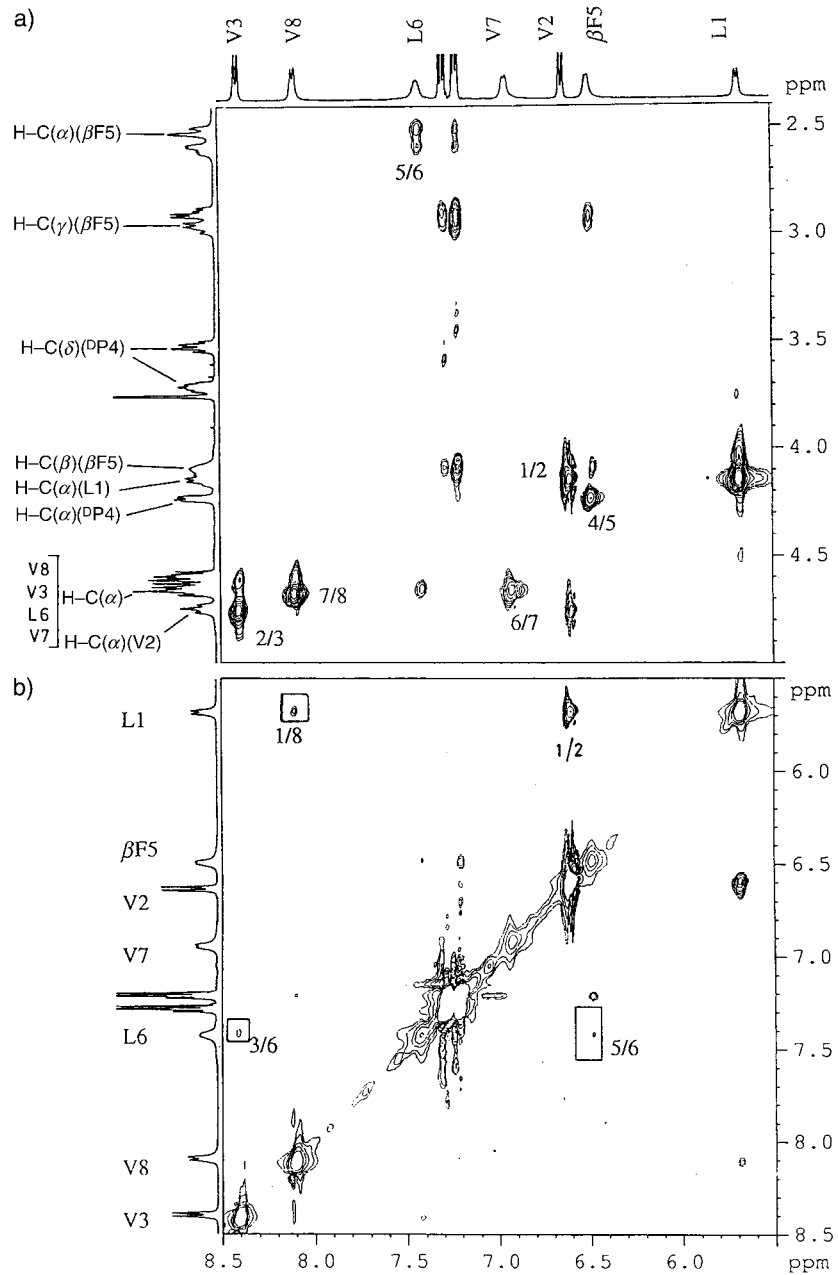


Fig. 4. Partial 500-MHz ROESY spectrum of peptide **1** in CDCl<sub>3</sub> at 300 K. a) H-C( $\alpha$ )  $\leftrightarrow$  N-H NOEs and b) N-H  $\leftrightarrow$  N-H NOEs. Cross-peaks are labelled with residue numbers. The long-range NOEs diagnostic of  $\beta$ -hairpin conformations are boxed.

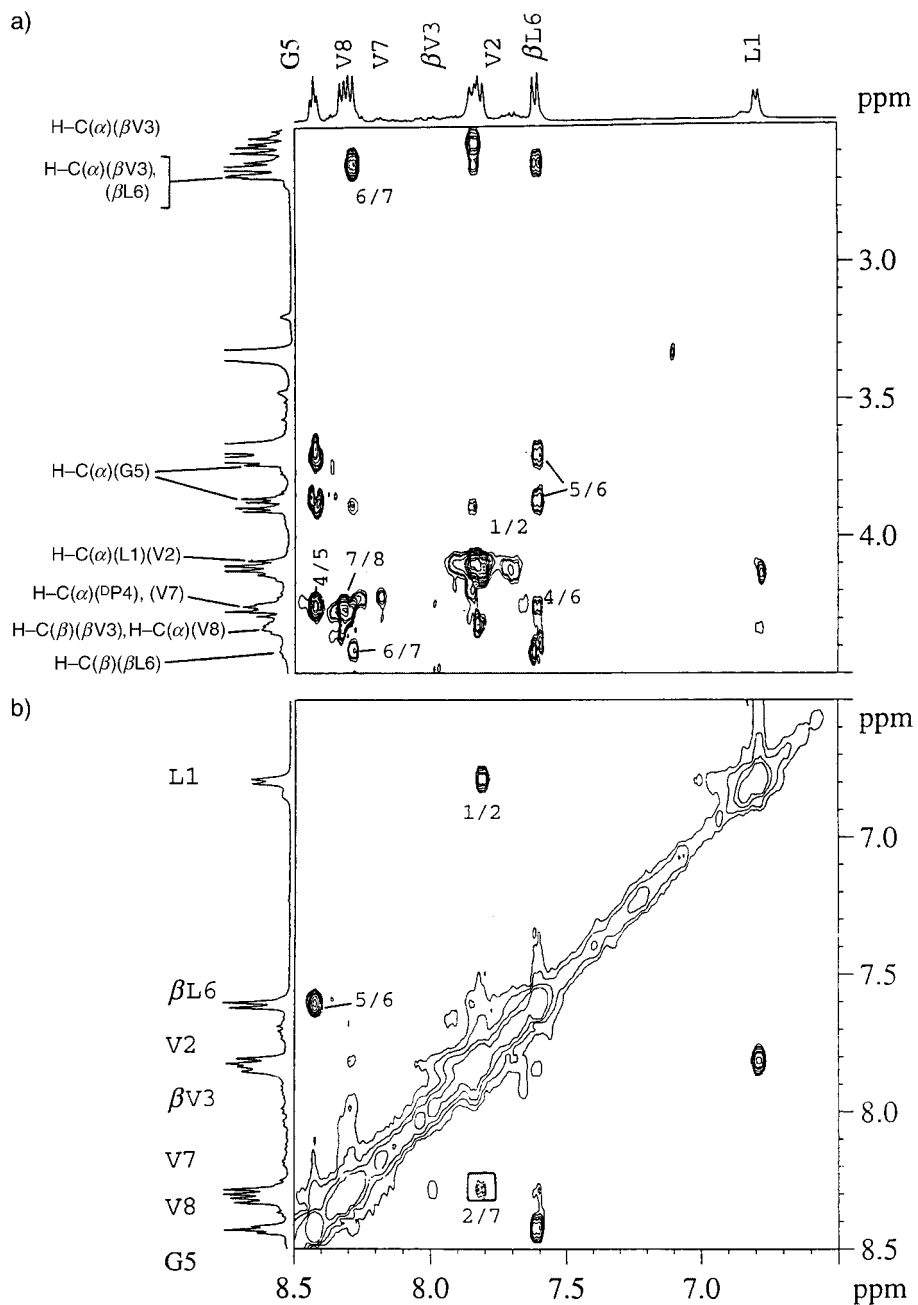


Fig. 5. Partial 500-MHz ROESY spectrum of peptide 2 in CD<sub>3</sub>OD at 300 K. a) H-C( $\alpha$ )  $\leftrightarrow$  N-H NOEs and b) N-H  $\leftrightarrow$  N-H NOEs. Cross-peaks are labelled with residue numbers. The long-range NOEs diagnostic of  $\beta$ -hairpin conformations are boxed.

Table 2.  $^1\text{H-NMR}$  (500 MHz) Chemical Shifts for Peptide **2** at 300 K in  $\text{CD}_3\text{OD}$ 

Residue	N–H	H–C( $\alpha$ )	H–C( $\beta$ )	Others
Leu(1)	6.79	4.13	1.68	1.56 (H–C( $\gamma$ )); 0.96 (2 Me( $\delta$ ))
Val(2)	7.81	0.13	2.03	0.96 (2 Me( $\gamma$ ))
$\beta$ Val(3)	7.84	2.58, 2.68	4.31	1.80 (H–C( $\gamma$ )); 0.98 (2 Me( $\delta$ ))
$^{\text{D}}$ Pro(4)		4.25	2.23	1.99, 2.12 ( $\text{CH}_2$ ( $\gamma$ )); 3.65, 3.73 ( $\text{CH}_2$ ( $\delta$ ))
Gly(5)	8.43	3.69, 3.89		
$\beta$ Leu(6)	7.61	2.42, 2.68	4.42	1.58 ( $\text{CH}_2$ ( $\gamma$ )); 1.28 (H–C( $\delta$ )); 0.90 (2 Me( $\epsilon$ ))
Val(7)	8.29	4.26	2.08	1.0 (2 Me( $\gamma$ ))
Val(8)	8.32	4.35	2.15	0.98 (2 Me( $\gamma$ ))

experiments. The chemical shifts are listed in Table 3. Fig. 6 shows sections of the ROESY spectrum illustrating conformationally relevant NOEs. The  $\beta$ -hairpin structure is supported by the observation of  $d_{\text{NN}}$  (4/7) and  $d_{\text{NN}}$  (1/10) connectivities. Further support for the hairpin comes from the observation of a strong  $d_{\alpha\alpha}$  (2/9) NOE (not shown) and the observation of a cross-strand NOE between N–H( $\beta$ Phe(3)) and H–C( $\beta$ )( $\beta$ Phe(8)).

Table 3.  $^1\text{H-NMR}$  (500 MHz) Chemical Shifts for Peptide **3** at 300 K in  $\text{CD}_3\text{OD}$ 

Residue	N–H	H–C( $\alpha$ )	H–C( $\beta$ )	Others
Leu(1)	6.80	4.18	1.72	1.69 (H–C( $\gamma$ )); 0.96 (2 Me( $\delta$ ))
Val(2)	7.74	4.55	1.98	0.90 (2 Me( $\gamma$ ))
$\beta$ Phe(3)	8.36	2.35, 2.95	4.68	2.7, 2.75 ( $\text{CH}_2$ ( $\gamma$ )); 7.10–7.26 (arom. H)
Val(4)	8.48	4.66	2.14	1.05 (2 Me( $\gamma$ ))
$^{\text{D}}$ Pro(5)		4.28	2.22	1.99, 2.12 ( $\text{CH}_2$ ( $\gamma$ )); 3.75, 3.80 ( $\text{CH}_2$ ( $\delta$ ))
Gly(6)	8.56	3.70, 3.88		
Leu(7)	8.20	4.41	1.79	1.69 (H–C( $\gamma$ )); 0.95 (2 Me( $\delta$ ))
$\beta$ Phe(8)	8.01	2.18, 2.35	4.32	2.69, 2.75 ( $\text{CH}_2$ ( $\gamma$ )); 7.10–7.26 (arom. H)
Val(9)	8.03	4.78	2.05	1.0 (2 Me( $\gamma$ ))
Val(10)	8.62	4.35	2.18	0.98 (2 Me( $\gamma$ ))

*Circular Dichroism.* Fig. 7 compares the far-UV/CD spectra of peptides **1–4**. In all cases, a strong negative band between 218 and 220 nm is observed, a feature seen in other peptide hairpins. The spectrum of peptides **3** shows evidence for additional bands seen as a shoulder at *ca.* 230 nm, presumably due to aromatic chromophores. Indeed, earlier studies of peptide hairpins have shown that far-UV/CD spectra can be considerably distorted as a consequence of through-space interactions between aromatic groups [32].

*Crystallographic Studies.* Single crystals suitable for X-ray diffraction were obtained for the peptides **2** and **3**, but peptide **1** has, thus far, remained recalcitrant to crystallization. The structure of peptide **3**, which adopts a  $\beta$ -hairpin conformation in crystals, has been reported earlier [33]. The crystal structure of peptide **2** is described below.

*Crystal Structure of Peptide 2.* Fig. 8 shows the conformation of peptide **3** in the crystal. Backbone and side-chain torsion angles and H-bond parameters are



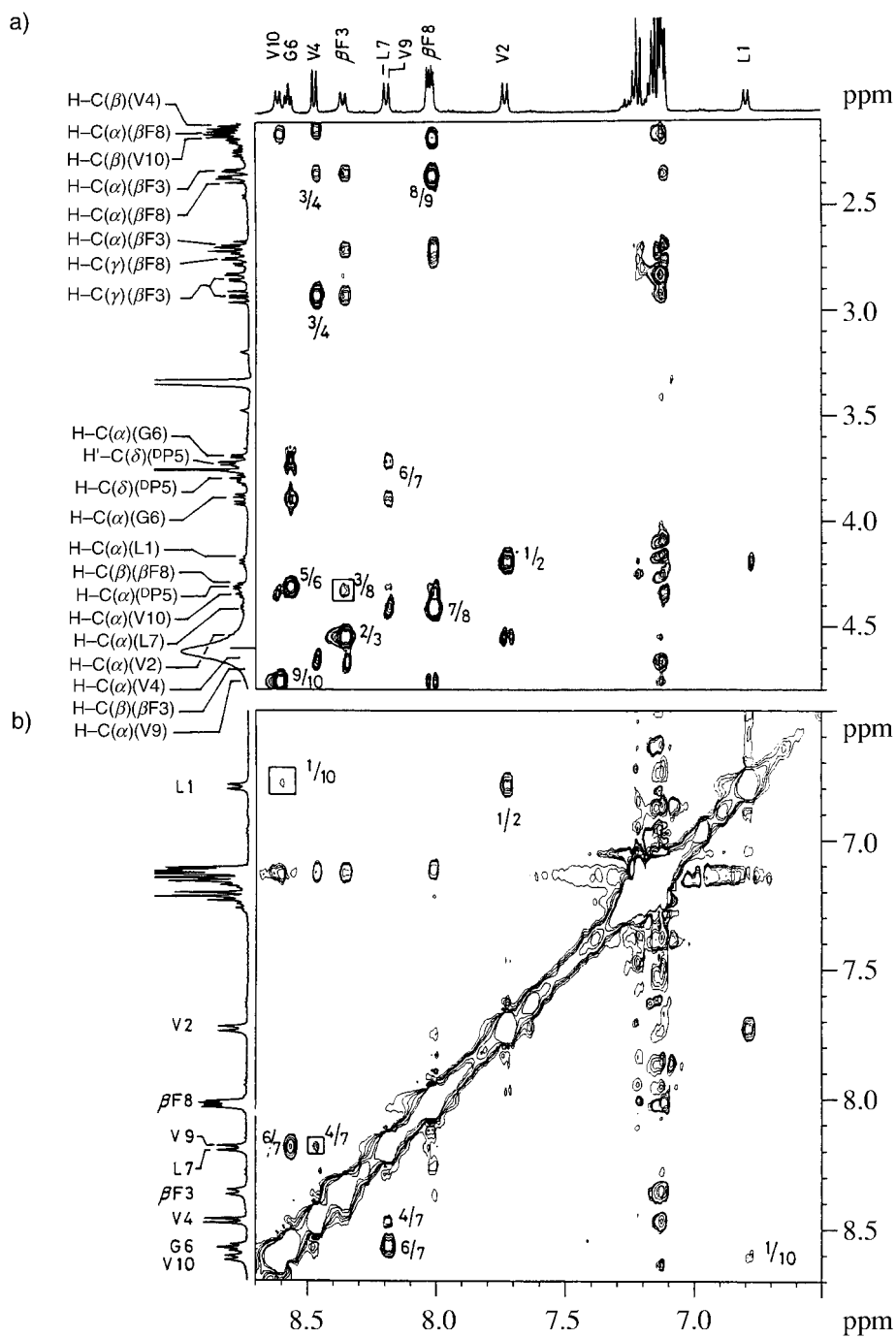


Fig. 6. Partial 500-MHz ROESY spectrum of peptide **3** in  $CD_3OD$  at 300 K. a) H-C( $\alpha$ )  $\leftrightarrow$  N-H NOEs and b) N-H  $\leftrightarrow$  N-H NOEs. Cross-peaks are labelled with residue numbers. The long-range NOEs diagnostic of  $\beta$ -hairpin conformations are boxed.

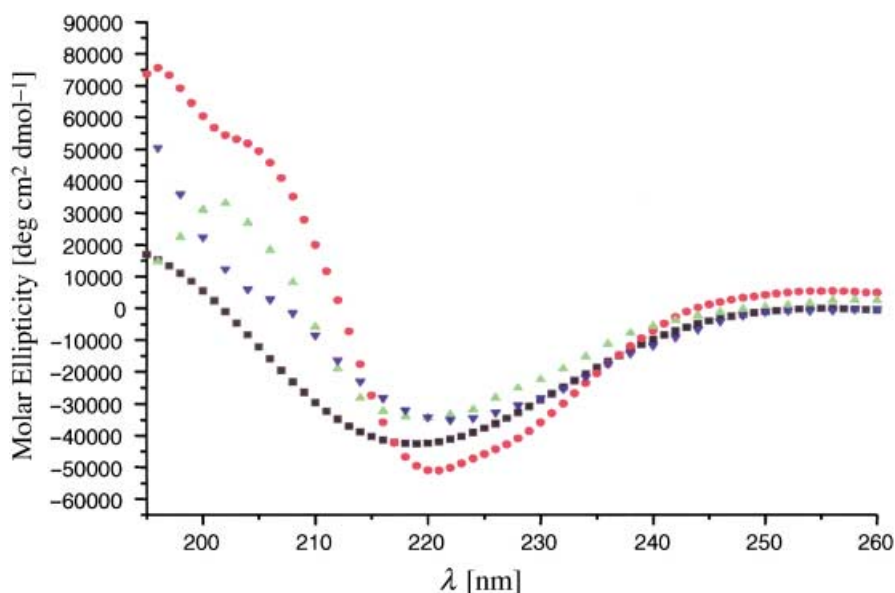


Fig. 7. Circular dichroism spectra of peptides **1** ( $\nabla$ ), **2** ( $\blacktriangle$ ), **3** ( $\bullet$ ), and **4** ( $\blacksquare$ ) in the far-UV region in MeOH

summarized in *Tables 4* and *5*, respectively. The molecule forms a  $\beta$ -hairpin with four cross-strand H-bonds. The  $^{\text{D}}\text{Pro-Gly}$  segment occurs in a type-I' conformation. The inspection of backbone torsion angles in *Table 4* reveals that the  $\beta\text{Val}(3)$  residue adopts an unusual *gauche* conformation ( $\theta_3 = +65^\circ$ ). Normally, in a strand position, a *trans* conformation ( $\theta = \pm 180^\circ$ ) would be anticipated for the  $\beta$ -residues. An almost completely extended value is obtained for  $\psi_3$  ( $-175^\circ$ ) of  $\beta\text{Val}(3)$ . Clearly, the distortion at  $\theta_3$  has been compensated by a corresponding change in  $\psi_3$  to maintain an antiparallel  $\beta$ -sheet. It should be noted that, for  $\beta$ -residues in the strand positions of hairpins, values of  $\phi$ ,  $\theta$ , and  $\psi$  are generally in the range of  $-120^\circ \pm 20^\circ$ ,  $+150^\circ \pm 30^\circ$ , and  $+120^\circ \pm 20^\circ$ , respectively, based on a limited number of known crystalline hairpins, containing both  $\alpha$ - and  $\beta$ -amino acid residues.

*Comparison of  $\beta$ -Hairpin-Containing  $\beta$ -Residues.* The availability of crystalline structures for peptide **2** (this study), **3** [33], and **4** [31] permits a comparison of conformational features and hairpin-packing arrangements. These, in turn, may be compared with the previously determined structure of the  $\alpha$ -peptide  $\beta$ -hairpin **4**. In peptide **4** (containing all  $\alpha$ -amino acids in the strand) and **5** ( $\beta$ -amino acids), the  $^{\text{D}}\text{Pro-Gly}$  segment adopts the type-II' conformation (idealized torsion angles are  $\phi_{\text{DPro}} = +60^\circ$ ,  $\psi_{\text{DPro}} = -120^\circ$ ,  $\phi_{\text{Gly}} = -80^\circ$ , and  $\psi_{\text{Gly}} = 0^\circ$ ). In contrast, for strands containing both  $\alpha$ - and  $\beta$ -amino acids, as in the case of peptide **2** and **3**, a type-I'  $\beta$ -turn conformation (idealized torsion angles are  $\phi_{\text{DPro}} = +60^\circ$ ,  $\psi_{\text{DPro}} = +30^\circ$ ,  $\phi_{\text{Gly}} = +90^\circ$ , and  $\psi_{\text{Gly}} = 0^\circ$ ) is obtained for  $^{\text{D}}\text{Pro-Gly}$  segments. A view of the molecular conformations observed in crystals of the peptides **2**, **3**, and **5** is shown in *Fig. 9*. Notably, in the  $\beta$ -hairpins in proteins, necessarily composed of only  $\alpha$ -amino acids, the extent of strand twist is determined by the nature of the nucleating  $\beta$ -turn. The hairpins

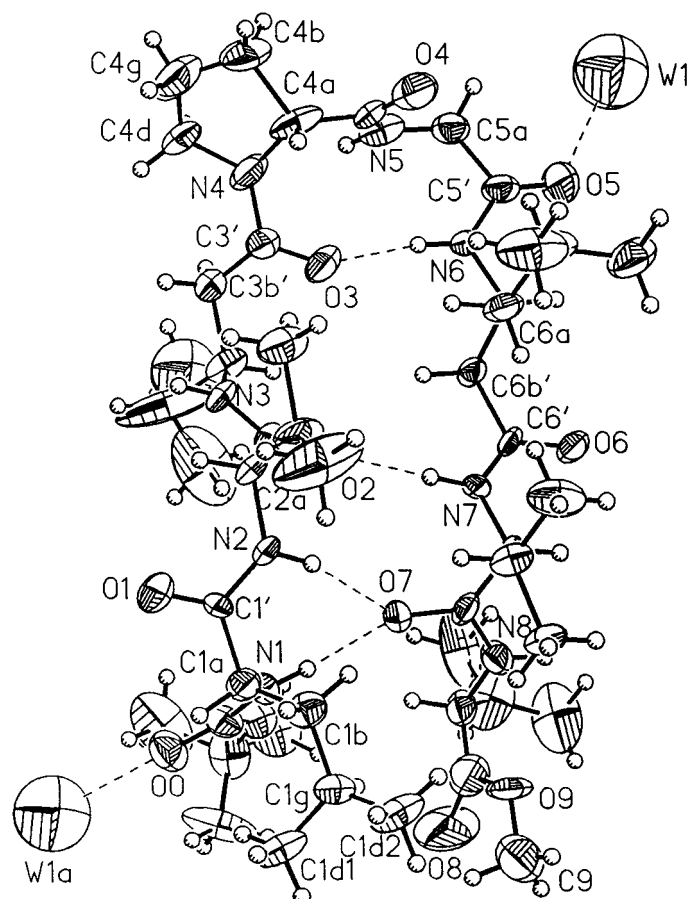


Fig. 8. ORTEP View of  $\beta$ -hairpin of **2**. Thermal ellipsoids are at 20% probability and the size of the H-atoms is arbitrary. Dotted lines represent H-bonds. W1 and W1a are symmetry-related H<sub>2</sub>O molecules.

nucleated by the type-II' turns are flatter, while those forming type-I' turns show a greater degree of strand twist [34].

The assemblies of  $\beta$ -sheets from individual molecules also separate into two general groups. Hairpins **4** and **5** assemble into extended  $\beta$ -sheets by simple lateral translation of molecules and intermolecular H-bonding, as shown in Fig. 10. The main difference between the sheets of **4** and **5** are the directions of the NH $\cdots$ O=C H-bonds. In **4**, the direction alternates along the strands, whereas in **5** all the C=O moieties point to the right and the direction of all H-bonds is the same. The unique directionality of the H-bonds implies a distinct polarity for the sheets [18][25][27].

The assembly of hairpins with mixed  $\alpha/\beta$ -residues, as exemplified by peptides **2** and **3**, falls into a different pattern (Fig. 11). Neighboring hairpins are related by a 2-fold rotation axis for **2** and a 2-fold screw axis for **3**. In each case, the  $\beta$ -turns in adjacent molecules alternate between top and bottom. The direction of individual C=O moieties depends upon the position of the  $\beta$ -residues in the strand, hence, the polar

Table 4. *Torsional Angles in Peptide 2*

Residue	Backbone		Side chains	
	Angle	[°]	Angle	[°]
Leu(1)	$\phi_1$	– 108	$\chi_{11}$	– 59
	$\psi_1$	– 52	$\chi_{12}$	– 47, – 176
	$\omega_1$	+ 178		
Val(2)	$\phi_2$	– 132	$\chi_{21}$	– 37, + 178
	$\psi_2$	+ 131		
	$\omega_2$	+ 178		
$\beta$ Val(3)	$\phi_3$	– 131	$\chi_{31}$	– 73, + 177
	$\theta_3$	+ 65		
	$\psi_3$	– 175		
<sup>D</sup> Pro(4)	$\omega_3$	+ 171		
	$\phi_4$	+ 70	$\chi_{41}$	+ 20
	$\psi_4$	+ 17	$\chi_{42}$	– 31
	$\omega_4$	– 174	$\chi_{43}$	– 11
Gly(5)			$\chi_{44}$	+ 26
	$\phi_5$	+ 73	$C(\delta)-N-C(\alpha)-C(\beta)$	– 5
	$\psi_5$	+ 17		
	$\omega_5$	+ 176		
$\beta$ Leu(6)	$\phi_6$	– 136	$\chi_{61}$	– 71
	$\theta_6$	– 178	$\chi_{62}$	– 67, – 173
	$\psi_6$	+ 115		
	$\omega_6$	– 179		
Val(7)	$\phi_7$	– 121	$\chi_{71}$	– 64, + 174
	$\psi_7$	+ 126		
	$\omega_7$	– 172		
Val(8)	$\phi_8$	– 109	$\chi_{81}$	– 79, + 69
	$\psi_8$	+ 1		
	$\omega_8$	+ 179		

Table 5. *H-Bonds in Peptide 2*

H-Bond type	Donor <sup>a)</sup>	Acceptor <sup>a)</sup>	$d(D \cdots A)$ [Å]	$d(H \cdots A)$ [Å] <sup>b)</sup>	$D \cdots O=C$ angle [°]
Intramol.	N(1)	O(7)	2.81	1.93	157
Intramol.	N(2)	O(7)	3.15	2.30	140
Intermol.	N(3)	O(1) <sup>c)</sup>	2.96	2.08	143
Intermol.	N(5)	O(4) <sup>d)</sup>	3.08	2.39	156
Intramol.	N(6)	O(3)	2.84	1.98	137
Intramol.	N(7)	O(2)	2.85	2.01	148
Intermol.	N(8)	O(6) <sup>e)</sup>	2.91	2.04	156
Solv.-pept.	W1	O(5)	2.69		123
Solv.-pept.	W1	O(0) <sup>f)</sup>	2.80		149

<sup>a)</sup> For assignments, see Fig. 8. <sup>b)</sup> H-Atoms were placed in idealized positions with  $N-H=0.90$  Å. <sup>c)</sup> At symmetry equivalent  $-x, +y, -z$ . <sup>d)</sup> At symmetry equivalent  $-1/2-x, +1/2+y, -z$ . <sup>e)</sup> At symmetry equivalent  $-x, +y, 1-z$ . <sup>f)</sup> At symmetry equivalent  $-1/2+x, -1/2+y, +z$ .

regions or bonds are scattered. In these four structures, the  $NH \cdots O=C$  H-bonds, both inside a hairpin and between hairpins, form loops of 10- or 14-membered rings, except for one 12-membered ring in **3** that contains the  $N(2)-H \cdots O(6b)$  and  $N(8b)-H \cdots O(2)$

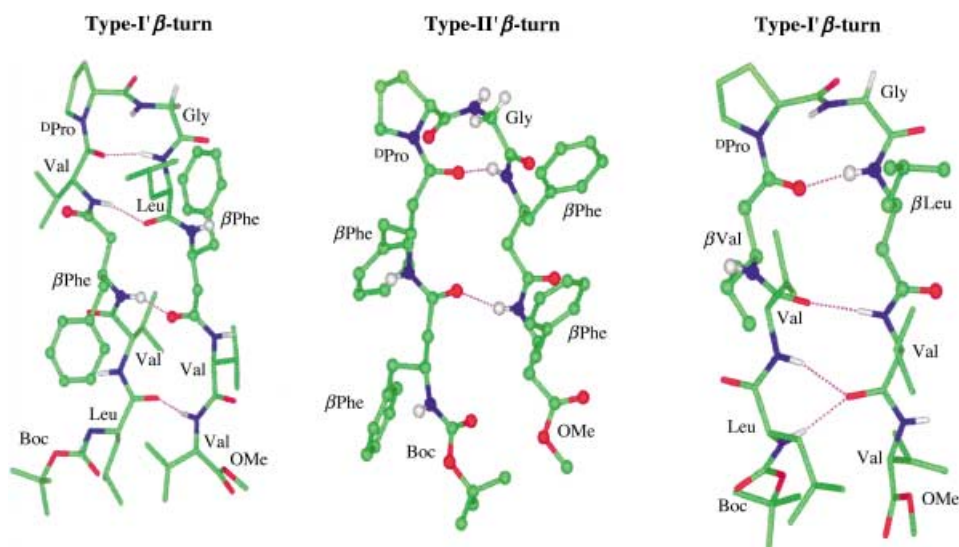


Fig. 9. Molecular structures of peptides **3** [33], **5** [31], and **2** (this study) determined by X-ray diffraction. These figures were generated by means of MOLMOL, with atomic coordinates obtained from X-ray data.

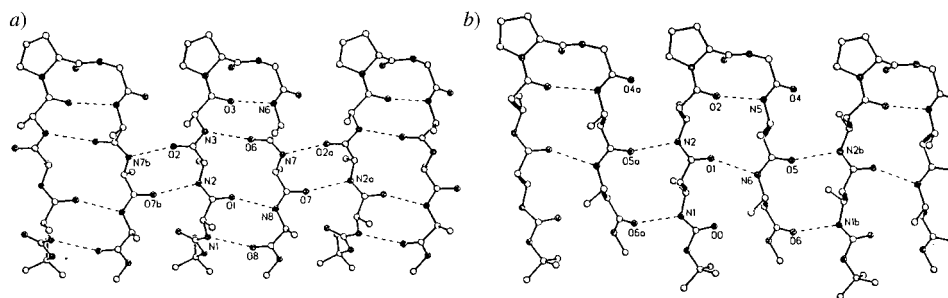


Fig. 10. a) Extended  $\beta$ -sheet of **4**.  $\text{NH} \cdots \text{O}=\text{C}$  H-bonds alternate directions and produce an apolar sheet [30]. b) Extended  $\beta$ -sheet of peptide **5**.  $\text{NH} \cdots \text{O}=\text{C}$  H-bonds all point in the same direction and produce a polar sheet [31].

H-bonds. All H-bonds are quite normal in length and direction. Table 5 lists the H-bond parameters for **2**.

The structures of hairpins **1–5** suggest that variations in the location of  $\beta$ -residues in the sequence of peptides that tend to form  $\beta$ -sheets can lead to  $\beta$ -sheets that have individualized polar properties.

**Conclusions.** – Results of our ongoing studies on  $\alpha/\beta$ -hybrid peptides suggest that  $\beta$ -residues can be accommodated into the turn and strand positions of the  $\beta$ -hairpins derived from parent  $\alpha$ -amino acid sequences. NMR and crystallographic evidence for hairpin structures in several model sequences provides strong support for this conclusion. The insertion of  $\beta$ -residues into extended strands alters the polarity of the

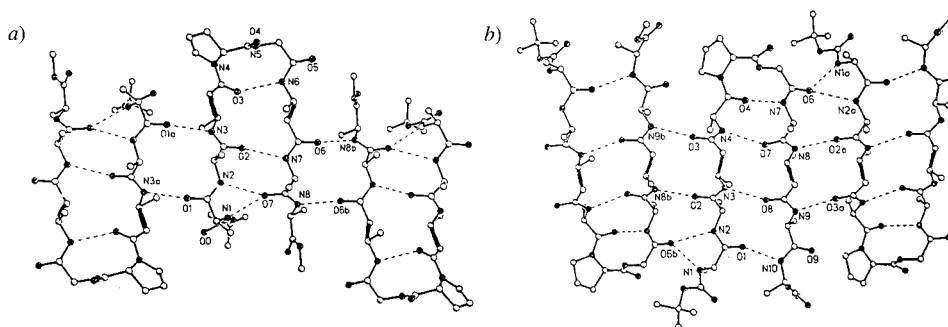


Fig. 11. a) Mixed  $\alpha/\beta$ -residues in the extended  $\beta$ -sheet of peptide **2** with scattered polar regions. b) Mixed  $\alpha/\beta$ -residues in the extended  $\beta$ -sheet of peptide **3** with a central polar band [33].

H-bond pattern both within the molecule and in the crystals. The orientation of the side chains with respect to the sheet scaffold are also altered. The insertion of chiral and multiply-substituted  $\beta$ -amino acids into peptides of defined structure is likely to provide many new opportunities for the creation of novel structures.

We thank *B. S. Sanjeev* and *S. Aravinda* for help in generating *Figs. 1* and *9*. This work was supported in Bangalore by a program grant in the area of Drug and Molecular Design by the *Department of Biotechnology*, Government of India. The work at the *Naval Research Laboratory* was supported by the *National Institute of Health*, Grant GM30202, and the *Office of Naval Research*.

#### Experimental Part

1. *General*. Abbreviations: Boc = (*tert*-butoxy)carbonyl, DCC = *N,N*-dicyclohexylcarbodiimide, HOBT = 1-hydroxybenzotriazole. THF and Et<sub>3</sub>N were refluxed over Na and distilled. Boc-amino acids were prepared with Boc anhydride. Diazomethane (CH<sub>2</sub>N<sub>2</sub>) gas was generated from *N*-methyl-(4-methylphenyl)-*N*-nitrosulfonamide. DMF was distilled over P<sub>2</sub>O<sub>5</sub>. Anal. HPLC: *Shimadzu SPD-6A* HPLC system (variable wavelength monitor). MPLC: *Büchi 684* with *Knauer* UV monitor. Semiprep. HPLC: *Hewlett-Packard Series 1100* system. CD: *Jasco J-715*, 1-mm cell length. NMR: *Bruker DRX-500*. MALDI-TOF-MS: *Kratos*.

2. *Synthesis of  $\beta$ -Amino Acids*. 2.1. *General Procedure*. According to literature procedures [11][35], the Boc-protected amino acid (10 mmol) was dissolved in anhyd. THF (25 ml) and then cooled to  $-15^\circ$ . Et<sub>3</sub>N (1.25 ml, 1 equiv.) and ClCOEt (1.25 ml, 1 equiv.) were added to the soln. After 30 min, a sat. soln. of CH<sub>2</sub>N<sub>2</sub> in CHCl<sub>3</sub> (650 ml) was added until intensive greenish-yellow color persisted. The mixture was then stirred for 5 h. After aq. workup by successive washing with 5% HCl (3  $\times$  50 ml), 5% NaHCO<sub>3</sub> (3  $\times$  50 ml), and brine (30 ml), the org. layer was concentrated under reduced pressure. The crude product was subjected to *Wolff* rearrangement.

As reported in [36], the diazoketone (10 mmol) was dissolved in THF (25 ml) with the addition of 10% (*v/v*) H<sub>2</sub>O and then cooled to  $-15^\circ$ . The soln. of AcOAg (1 mmol) in Et<sub>3</sub>N (11 mmol) was added, and the resulting mixture was stirred for 3 h. The progress of the reaction was monitored by TLC (CHCl<sub>3</sub>/MeOH/AcOH 40 : 2 : 1 (*v/v/v*)). The solvent was removed under reduced pressure, and the residue was diluted with H<sub>2</sub>O. The aq. phase was extracted with AcOEt, and the resulting colorless phase was adjusted to pH 2 with 2*N* HCl and extracted with AcOEt. The AcOEt extracts were washed with brine, dried (Na<sub>2</sub>SO<sub>4</sub>), and the solvent was removed under reduced pressure.

2.2. (*S*)-3-[(*tert*-Butoxy)carbonyl]amino]-4-phenylbutanoic Acid (Boc- $\beta$ Phe). According to 2.1, reaction with Boc-(*S*)-phenylalanine (7.95 g, 30 mmol) gave, after aq. workup, 7.5 g (86%) of the corresponding diazoketone as yellow crystalline needles.

According to 2.1, reaction with *tert*-butyl *N*-[(*S*)-1-benzyl-3-diazenyl-2-oxopropyl]carbamate (7.2 g, 25 mmol) gave, after workup, 5.3 g (76%) of Boc- $\beta$ Phe as a white solid. <sup>1</sup>H-NMR (80 MHz, CDCl<sub>3</sub>): 1.42 (*s*, *t*-Bu); 2.42 (*d*, CH<sub>2</sub>); 2.86 (*d*, CH<sub>2</sub>); 4.45 (*m*, CH), 7.25 (*s*, arom. H).

2.3. (R)-3-[[tert-Butoxy]carbonyl]amino]-4-methylpentanoic Acid (Boc- $\beta$ Val). According to 2.1, reaction with Boc-(S)-valine (8.68 g, 40 mmol) gave, after aq. workup, 8.3 g (86%) of the corresponding diazoketone as yellow crystalline needles.

According to 2.1, reaction with *tert*-butyl *N*-[(S)-1-diazenyl-1-isopropyl-2-oxopropyl]carbamate (8.0 g) gave, after workup, 5.6 g (73%) of Boc- $\beta$ Val as a white solid. <sup>1</sup>H-NMR (80 MHz, CDCl<sub>3</sub>): 0.92 (*d*, 2 Me); 1.38 (*s*, *t*-Bu); 2.22 (*m*, CH); 2.36 (*d*, CH<sub>2</sub>); 4.20 (*m*, CH).

2.4. (S)-3-[[tert-Butoxy]carbonyl]amino]-5-methylhexanoic Acid (Boc- $\beta$ Leu). According to 2.1, reaction with Boc-(S)-leucine (9.24 g, 40 mmol) gave, after aq. workup, 8.6 g (85%) of the corresponding diazoketone as yellow crystalline needles.

According to 2.1, reaction with *tert*-butyl *N*-[(S)-1-(2-diazenyl-1-oxoethyl)-3-methylbutyl]carbamate (8.3 g) gave, after workup, 6.2 g of Boc- $\beta$ Leu as a white solid. <sup>1</sup>H-NMR (80 MHz, CDCl<sub>3</sub>): 0.90 (*d*, 2 Me); 1.38 (*s*, *t*-Bu); 1.56 (*m*, CH); 1.65 (*m*, CH<sub>2</sub>); 2.45 (*d*, CH<sub>2</sub>); 4.20 (*m*, CH).

2.5. Methyl (R)-3-[[tert-Butoxy]carbonyl]amino]-4-methylpentanoate (Boc- $\beta$ Val-OMe). Boc- $\beta$ Val (2.31 g, 10 mmol) was dissolved in MeOH (5 ml) and diluted with 100 ml of Et<sub>2</sub>O. CH<sub>3</sub>N<sub>2</sub> was passed to the soln. until it turned yellow. Et<sub>2</sub>O was evaporated under reduced pressure to yield 2.25 g (92%) of Boc- $\beta$ Val-OMe. <sup>1</sup>H-NMR (80 MHz, CDCl<sub>3</sub>): 0.90 (*d*, 2 Me); 1.38 (*s*, *t*-Bu); 2.22 (*m*, CH); 2.36 (*d*, CH<sub>2</sub>); 3.61 (*s*, OMe); 4.20 (*m*, CH).

2.6. Methyl (S)-3-[[tert-Butoxy]carbonyl]amino]-4-phenylbutanoate (Boc- $\beta$ Phe-OMe). Synthesized with Boc- $\beta$ Phe according to 2.5. <sup>1</sup>H-NMR (80 MHz, CDCl<sub>3</sub>): 1.43 (*s*, *t*-Bu); 2.45 (*d*, CH<sub>2</sub>); 2.86 (*d*, CH<sub>2</sub>); 3.60 (*s*, MeO); 4.45 (*m*, CH); 7.25 (*s*, arom. H).

3. Synthesis of Peptides Containing  $\alpha$ - and  $\beta$ -Amino Acids. Peptides **1**, **2**, and **3** were synthesized by conventional solution-phase methods, by means of a fragment condensation strategy. The Boc-group was used for N-terminal protection, and the C-terminus was protected as a methyl ester. Deprotections were performed with 98–100% HCOOH and saponification for the N- and C-terminal protecting groups, resp. (monitored by TLC). Couplings were mediated by DCC/HOBt (1.01 equiv.). All intermediates were characterized by <sup>1</sup>H-NMR (80 MHz) and TLC (SiO<sub>2</sub>, CHCl<sub>3</sub>/MeOH 9:1 (*v/v*)) and were used without further purification. The final peptides were purified by reversed-phase MPLC (C<sub>18</sub>-column, 40–60  $\mu$ m, MeOH/H<sub>2</sub>O 60:40–95:5) and then by reversed-phase HPLC (C<sub>18</sub>-column, 5–10  $\mu$ m, MeOH/H<sub>2</sub>O gradients). The homogeneity of the purified peptides were ascertained by anal. HPLC. The purified peptides were characterized by MALDI-TOF-MS and by assignment of the 500-MHz <sup>1</sup>H-NMR spectra.

3.1. Synthesis of Boc-Leu-Val-Val-<sup>o</sup>Pro- $\beta$ Phe-Leu-Val-Val-OMe (**1**). 3.1.1. Boc-Val-Val-OMe. Boc-Val (5.4 g, 25 mmol) was dissolved in CH<sub>2</sub>Cl<sub>2</sub> (20 ml) and cooled in an ice bath. H-Val-OMe, isolated from 8.4 g (50 mmol) of H-Val-OMe·HCl, was added to the mixture followed by 5.4 g (27 mmol) of DCC. The mixture was allowed to warm to r.t. and stirred for 6 h. CH<sub>2</sub>Cl<sub>2</sub> was evaporated, and the residue was taken up in 100 ml of AcOEt. The precipitated dicyclohexyl urea (DCU) was filtered off. The filtrate was washed with 2*N* HCl (3  $\times$  50 ml), 5% Na<sub>2</sub>CO<sub>3</sub> (3  $\times$  50 ml), brine (50 ml), and dried (Na<sub>2</sub>SO<sub>4</sub>). The org. layer was evaporated under reduced pressure to yield 8 g (95%) of Boc-Val-Val-OMe as a white solid. <sup>1</sup>H-NMR (80 MHz, CDCl<sub>3</sub>): 0.95 (*m*, 4 Me(Val)); 1.46 (*s*, *t*-Bu); 2.15 (*m*, 2 H-C( $\beta$ )(Val)); 3.7 (*s*, MeO); 3.85 (*m*, H-C( $\alpha$ )(Val(1))); 4.5 (*m*, H-C( $\alpha$ )(Val(2))); 5.0 (*d*, NH(Val(1))); 6.35 (*d*, NH(Val(2))).

3.1.2. Boc-Leu-Val-Val-OMe. Boc-Val-Val-OMe (4.9 g, 15 mmol) was deprotected with 60 ml of HCOOH. After 4 h, HCOOH was evaporated, and the residue was diluted with 100 ml of H<sub>2</sub>O. The aq. soln. was washed with Et<sub>2</sub>O (3  $\times$  30 ml). The pH of the aq. layer was adjusted to ca. 9.0 with Na<sub>2</sub>CO<sub>3</sub>, and the resulting soln. was extracted with AcOEt (3  $\times$  50 ml). The combined AcOEt extract was washed with brine (30 ml), dried (Na<sub>2</sub>SO<sub>4</sub>), and concentrated under reduced pressure to ca. 10 ml. The soln. was added to a pre-cooled soln. of 3.7 g (16 mmol) of Boc-Leu in 15 ml of anhyd. DMF. After coupling (DCC/HOBT), the mixture was kept at r.t. for 16 h. DCU was filtered off after diluting with 100 ml of AcOEt, and the filtrate was subsequently washed with 2*N* HCl (3  $\times$  20 ml), 5% Na<sub>2</sub>CO<sub>3</sub> (3  $\times$  20 ml), and brine (30 ml). The org. layer was dried (Na<sub>2</sub>SO<sub>4</sub>) and evaporated under reduced pressure to yield 4.6 g (70%) of Boc-Leu-Val-Val-OMe as a white solid. <sup>1</sup>H-NMR (80 MHz, CDCl<sub>3</sub>): 0.90 (*m*, 2 Me(Leu), 4 Me(Val)); 1.44 (*s*, *t*-Bu); 1.56 (*m*, CH<sub>2</sub>( $\beta$ )(Leu), H-C(Leu)); 2.1 (*m*, 2 H-C( $\beta$ )(Val)); 3.72 (*s*, MeO); 4.1 (*m*, H-C( $\alpha$ )(Leu)); 4.4 (*m*, 2 H-C( $\alpha$ )(Val)); 5.3 (*d*, NH(Leu)); 6.35 (*d*, NH(Val)); 6.65 (*d*, NH(Val)).

3.1.3. Boc-Leu-Val-Val-OH. Boc-Leu-Val-Val-OMe (2.8 g, 6.5 mmol) was dissolved in 25 ml of MeOH, and 14 ml of 1*N* NaOH was added slowly. After 8 h, MeOH was evaporated under reduced pressure, the residue was dissolved in 30 ml of H<sub>2</sub>O and washed with Et<sub>2</sub>O (3  $\times$  20 ml). The aq. soln. was cooled in an ice bath, acidified with 1*N* HCl to pH 2, and extracted with AcOEt (3  $\times$  30 ml). The combined AcOEt extract was dried (Na<sub>2</sub>SO<sub>4</sub>) and evaporated to yield 2.6 g (92%) of Boc-Leu-Val-Val-OH as a white solid.

3.1.4. *Boc-βPhe-Leu-Val-Val-OMe*. Boc-Leu-Val-Val-OMe (2.2 g, 5 mmol) was deprotected with 20 ml of HCOOH. After 4 h, HCOOH was evaporated, and the residue was diluted with 100 ml of H<sub>2</sub>O. After aq. workup according to 3.1.2, the org. layer was concentrated to ca. 5 ml and was added to a pre-cooled soln. of 1.4 g (5 mmol) of Boc-βPhe in 8 ml of anh. DMF. After coupling (DCC/HOBT), the mixture was kept at r.t. for 20 h. Workup according to 3.1.2 yielded 2.1 g (70%) of Boc-βPhe-Leu-Val-Val-OMe as a white solid. <sup>1</sup>H-NMR (80 MHz, CDCl<sub>3</sub>): 0.90 (*m*, 2 Me(Leu), Me(Val)); 1.44 (*s*, *t*-Bu); 1.56 (*m*, CH<sub>2</sub>(β)(Leu), H-C(γ)(Leu)); 2.1 (*m*, 2 H-C(β)(Val)); 2.42 (*d*, CH<sub>2</sub>(α)(βPhe)); 2.85 (*d*, CH<sub>2</sub>(γ)(βPhe)); 3.72 (*s*, MeO); 4.1–4.6 (*m*, 3 H-C(α)(Leu,Val,Val), H-C(β)(βPhe)); 5.3, 6.75, 6.9 (3*d*, 3 NH); 7.23 (*s*, 5 arom. H); 7.5 (*d*, NH).

3.1.5. *Boc-<sup>D</sup>Pro-βPhe-Leu-Val-Val-OMe*. Boc-βPhe-Leu-Val-Val-OMe (1.8 g, 3 mmol) was deprotected with 12 ml of HCOOH. After 4 h, HCOOH was evaporated, and the residue was diluted with 100 ml of H<sub>2</sub>O. After aq. workup according to 3.1.2, the org. phase was concentrated to 5 ml and was added to a pre-cooled soln. of 0.64 g (3 mmol) of Boc-<sup>D</sup>Pro in 5 ml of anh. DMF. After coupling (DCC/HOBT), the mixture was kept at r.t. for 36 h. Workup according to 3.1.2 yielded 1.35 g (65%) of Boc-<sup>D</sup>Pro-βPhe-Leu-Val-Val-OMe as a white solid. <sup>1</sup>H-NMR (80 MHz, CDCl<sub>3</sub>): 0.86 (*m*, 2 Me(Leu), 4 Me(Val)); 1.45 (*s*, *t*-Bu); 1.62 (*m*, CH<sub>2</sub>(β)(Leu), H-C(γ)(Leu)); 1.75–2.25 (*m*, 2 H-C(β)(Val), CH<sub>2</sub>(β)(<sup>D</sup>Pro), CH<sub>2</sub>(γ)(<sup>D</sup>Pro)); 2.45 (*d*, CH<sub>2</sub>(α)(βPhe)); 2.83 (*d*, CH<sub>2</sub>(γ)(βPhe)); 3.4 (*m*, CH<sub>2</sub>(δ)(<sup>D</sup>Pro)); 3.65 (*s*, MeO); 4.1–4.5 (*m*, 4 H-C(α)(Leu,<sup>D</sup>Pro,Val,Val), H-C(β)(βPhe)); 5.5, 6.5, 7.1 (3*d*, 3 NH); 7.25 (*s*, 5 arom. H); 7.4 (*d*, NH).

3.1.6. *Boc-Leu-Val-Val-<sup>D</sup>Pro-βPhe-Leu-Val-Val-OMe (1)*. Boc-<sup>D</sup>Pro-βPhe-Leu-Val-Val-OMe (0.6 g, 0.86 mmol) was deprotected with 4 ml of HCOOH. After aq. workup according to 3.1.2, the org. layer was concentrated to ca. 3 ml and was added to a pre-cooled soln. of 0.37 g (0.86 mmol) of Boc-Leu-Val-Val-OH in 5 ml of anh. DMF. After coupling (DCC/HOBT), the mixture was kept at r.t. for 2 d. Workup was achieved according to 3.1.2 to give crude **1** (0.6 g, 69%), which was purified by MPLC and then further purified by HPLC. <sup>1</sup>H-NMR (500 MHz): see Table 1. MALDI-TOF-MS: 1035.5 ([*M* + Na]<sup>+</sup>, calc. 1012).

3.2. *Synthesis of Boc-Leu-Val-βVal-<sup>D</sup>Pro-Gly-βLeu-Val-Val-OMe (2)*. 3.2.1. *Boc-βLeu-Val-Val-OMe*. Boc-Val-Val-OMe (2.6 g, 8 mmol) was deprotected with 32 ml of HCOOH. After 4 h, HCOOH was evaporated, and the residue was diluted with 100 ml of H<sub>2</sub>O. After aq. workup according to 3.1.2, the org. layer was concentrated to ca. 10 ml and was added to a pre-cooled soln. of 1.9 g (8.1 mmol) of Boc-βLeu in 10 ml of anh. DMF. After coupling (DCC/HOBT), the mixture was kept at r.t. for 14 h. Workup according to 3.1.2 yielded 2.7 g (75%) of Boc-βLeu-Val-Val-OMe as a white solid. <sup>1</sup>H-NMR (80 MHz, CDCl<sub>3</sub>): 0.91 (*m*, 2 Me(βLeu), 4 Me(Val)); 1.42 (*s*, *t*-Bu); 1.56–1.72 (*m*, CH<sub>2</sub>(γ)(βLeu), H-C(δ)(βLeu)); 1.89 (*m*, 2 H-C(β)(Val)); 2.42 (*d*, CH<sub>2</sub>(α)(βLeu)); 3.56 (*s*, MeO); 4.1–4.5 (*m*, 2 H-C(α)(Val), H-C(β)(βLeu)); 5.4, 6.75, 7.32 (3*d*, 3 NH).

3.2.2. *Boc-Leu-Val-βVal-OMe*. Boc-βVal-OMe (1.38 g, 6 mmol) was deprotected with 24 ml of HCOOH. After 4 h, HCOOH was evaporated, and the residue was diluted with 60 ml of H<sub>2</sub>O. After aq. workup according to 3.1.2, the org. layer was concentrated to ca. 10 ml and was added to a pre-cooled soln. of 1.32 g (4 mmol) of Boc-Leu-Val-OH in 5 ml of anh. DMF. After coupling (DCC/HOBT), the mixture was kept at r.t. for 12 h. Workup according to 3.1.2 yielded 1.2 g (63%) of Boc-Leu-Val-βVal-OMe as a white solid. <sup>1</sup>H-NMR (80 MHz, CDCl<sub>3</sub>): 0.91 (*m*, 2 Me(Leu), 2 Me(Val), 2 Me(βVal)); 1.44 (*s*, *t*-Bu); 1.56 (*m*, CH<sub>2</sub>(β)Leu), H-C(γ)(Leu)); 2.1 (*m*, H-C(β)(Val), H-C(γ)(βVal)); 2.36 (*d*, CH<sub>2</sub>(α)(βVal)); 3.62 (*s*, MeO); 4.1–4.5 (*m*, H-C(α)(Leu), H-C(α)(Val), H-C(β)(βVal)); 5.6, 6.65, 6.8 (3*d*, 3 NH).

3.2.3. *Boc-<sup>D</sup>Pro-Gly-βLeu-Val-Val-OMe*. Boc-βLeu-Val-Val-OMe (0.9 g, 2 mmol) was deprotected with 10 ml of HCOOH. After 4 h, HCOOH was evaporated, and the residue was diluted with 50 ml of H<sub>2</sub>O. After aq. workup according to 3.1.2, the org. layer was concentrated to ca. 6 ml and was added to a pre-cooled soln. of 0.54 g (2 mmol) of Boc-<sup>D</sup>Pro-Gly [37] in 6 ml of anh. DMF. After coupling (DCC/HOBT), the mixture was kept at r.t. for 20 h. Workup according to 3.1.2 yielded 0.9 g (75%) of Boc-βLeu-Val-Val-OMe as a white solid. <sup>1</sup>H-NMR (80 MHz, CDCl<sub>3</sub>): 0.86 (*m*, 2 Me(Leu), 4 Me(Val)); 1.42 (*s*, *t*-Bu); 1.56 (*m*, CH<sub>2</sub>(γ)(βLeu), H-C(δ)(βLeu)); 1.75–2.25 (*m*, 2 H-C(β)(Val), CH<sub>2</sub>(β)(<sup>D</sup>Pro), CH<sub>2</sub>(γ)(<sup>D</sup>Pro)); 2.42 (*d*, CH<sub>2</sub>(α)(βLeu)); 3.4–3.7 (*m*, CH<sub>2</sub>(δ)<sup>D</sup>Pro), CH<sub>2</sub>(α)(Gly)); 3.62 (*s*, MeO); 4.1–4.5 (*m*, 3 H-C(α)(<sup>D</sup>Pro,Val,Val), H-C(β)(βLeu)); 5.4, 6.55 (2*d*, 2 NH); 6.85 (*m*, NH); 7.3 (*d*, NH).

3.2.4. *Boc-Leu-Val-βVal-<sup>D</sup>Pro-Gly-βLeu-Val-Val-OMe (2)*. Boc-<sup>D</sup>Pro-Gly-βLeu-Val-Val-OMe (0.73 g, 1.2 mmol) was deprotected with 6 ml of HCOOH. After 4 h, HCOOH was evaporated, and the residue was diluted with 50 ml of H<sub>2</sub>O. After aq. workup according to 3.1.2, the AcOEt layer was concentrated under reduced pressure to ca. 3 ml and was added to a pre-cooled soln. of 0.53 g (1.2 mmol) of Boc-Leu-Val-βVal-OH in 6 ml of anh. DMF. After coupling (DCC/HOBT), the mixture was stirred at r.t. for 2 d. Workup according to 3.1.2 gave crude **2** (0.8 g, 72%), which was subjected to MPLC and was further purified by HPLC. <sup>1</sup>H-NMR (500 MHz): see Table 2. MALDI-TOF-MS: 960.8 ([*M* + Na]<sup>+</sup>, calc. 936).



3.3. *Synthesis of Boc-Leu-Val-βPhe-Val-<sup>D</sup>Pro-Gly-Leu-βPhe-Val-Val-OMe (3)*. 3.3.1. *Boc-Leu-Val-βPhe-Val-OMe*. Boc-βPhe-Val-OMe (1.54 g, 4 mmol) was deprotected with 12 ml of HCOOH. After 4 h, HCOOH was evaporated, and the residue was diluted with 80 ml of H<sub>2</sub>O. After aq. workup according to 3.1.2, the org. layer was concentrated to ca. 10 ml and was added to a pre-cooled soln. of 1.32 g (4 mmol) of Boc-Leu-Val-OH in 10 ml of anh. DMF. After coupling (DCC/HOBT), the mixture was kept at r.t. for 24 h. Workup according to 3.1.2 yielded 1.82 g (75%) of Boc-Leu-Val-βPhe-Val-OMe as a white solid. <sup>1</sup>H-NMR (80 MHz, CDCl<sub>3</sub>): 0.89 (*m*, 2 Me(Leu), 4 Me(Val)); 1.42 (*s*, *t*-Bu); 1.56 (*m*, CH<sub>2</sub>(β)(Leu), H-C(γ)(Leu)); 2.1 (*m*, 2 H-C(β)(Val)); 2.38 (*d*, CH<sub>2</sub>(α)(βPhe)); 2.85 (*d*, CH<sub>2</sub>(γ)(βPhe)); 3.62 (*s*, MeO); 4.1–4.6 (*m*, 3 H-C(α)(Leu,Val,Val), H-C(β)(βPhe)); 5.3 (*d*, NH(Leu)); 6.35, 6.65, 6.8 (3*d*, 3 NH); 7.25 (*s*, 5 arom. H).

3.3.2. *Boc-Leu-βPhe-Val-Val-OMe*. Boc-Val-Val-OMe (1.65 g, 5 mmol) was deprotected with 20 ml of HCOOH. After 4 h, HCOOH was evaporated, and the residue was diluted with 80 ml of H<sub>2</sub>O. After aq. workup according to 3.1.2, the org. layer was concentrated to ca. 10 ml and was added to a pre-cooled soln. of 3.7 g (5.1 mmol) of Boc-Leu-βPhe-OH in 15 ml of anh. AcOEt. After coupling (DCC/HOBT), the mixture was kept at r.t. for 48 h. Workup according to 3.1.2 yielded 2.4 g (80%) of Boc-Leu-βPhe-Val-Val-OMe as a white solid. <sup>1</sup>H-NMR (80 MHz, CDCl<sub>3</sub>): 0.86 (*m*, 2 Me(Leu), 4 Me(Val)); 1.44 (*s*, *t*-Bu); 1.56 (*m*, CH<sub>2</sub>(β)(Leu), H-C(γ)(Leu)); 2.1 (*m*, 2 H-C(β)(Val)); 2.42 (*d*, CH<sub>2</sub>(α)(βPhe)); 2.85 (*d*, CH<sub>2</sub>(γ)(βPhe)); 3.65 (*s*, MeO); 4.1–4.6 (*m*, 3 H-C(α)(Leu,Val,Val), H-C(β)(βPhe)); 5.5 (*d*, NH(Leu)); 6.63, 6.9 (2*d*, 2 NH), 7.28 (*s*, 5 arom. H); 7.45 (*d*, NH).

3.3.3. *Boc-<sup>D</sup>Pro-Gly-Leu-βPhe-Val-Val-OMe*. Boc-Leu-βPhe-Val-Val-OMe (2.5 g, 2.5 mmol) was deprotected with 10 ml of HCOOH. After 4 h, HCOOH was evaporated and the residue was diluted with 100 ml of H<sub>2</sub>O. After aq. workup according to 3.1.2, the org. phase was concentrated to 5 ml and was added to a pre-cooled soln. of 0.67 g (2.5 mmol) of Boc-<sup>D</sup>Pro-Gly in 10 ml of anh. DMF. After coupling (DCC/HOBT), the mixture was kept at r.t. for 48 h. Workup according to 3.1.2 yielded 1.9 g (60%) of Boc-<sup>D</sup>Pro-Gly-Leu-βPhe-Val-Val-OMe as a white solid. <sup>1</sup>H-NMR (80 MHz, CDCl<sub>3</sub>): 0.86 (*m*, 2 Me(Leu), 4 Me(Val)); 1.40 (*s*, *t*-Bu); 1.62 (*m*, CH<sub>2</sub>(β)(Leu), H-C(γ)(Leu)); 1.74–2.24 (*m*, 2 H-C(β)(Val), CH<sub>2</sub>(β)(<sup>D</sup>Pro), CH<sub>2</sub>(γ)(<sup>D</sup>Pro)); 2.45 (*d*, CH<sub>2</sub>(α)(βPhe)); 2.83 (*d*, CH<sub>2</sub>(γ)(βPhe)); 3.4 (*m*, CH<sub>2</sub>(δ)(<sup>D</sup>Pro), CH<sub>2</sub>(α)(Gly)); 3.65 (*s*, MeO); 4.1–4.5 (*m*, 4 H-C(α)(Leu,<sup>D</sup>Pro,Val,Val), H-C(β)(βPhe)); 5.5, 6.5, 7.1 (3*d*, 3 NH); 7.25 (*s*, 5 arom. H); 7.35 (*t*, NH(Gly)); 7.4 (*d*, NH).

3.3.4. *Boc-Leu-Val-βPhe-Val-<sup>D</sup>Pro-Gly-Leu-βPhe-Val-Val-OMe (3)*. Boc-<sup>D</sup>Pro-Gly-Leu-βPhe-Val-Val-OMe (0.75 g, 1 mmol) was deprotected with 4 ml of HCOOH. After 6 h, HCOOH was evaporated, and the residue was diluted with 120 ml of H<sub>2</sub>O. After aq. workup according to 3.1.2, the AcOEt layer was concentrated under reduced pressure to ca. 6 ml and was then added to a pre-cooled soln. of 0.59 g (1 mmol) of Boc-Leu-Val-βPhe-Val-OH in 6 ml of anh. DMF. HOBT (0.16 g, 1.1 mmol) was used for coupling. The mixture was stirred at r.t. for 3 d. Workup was achieved as described in 3.1.2 to give crude **3** (0.85 g, 70%), which was subjected to MPLC and was further purified by HPLC. <sup>1</sup>H-NMR (500 MHz): see Table 3. MALDI-TOF-MS: 1252.3 ([*M* + Na]<sup>+</sup>, calc. 1232.5).

3.4. *X-Ray Crystallography*. Single crystals were obtained by slow evaporation from MeOH. A colorless crystal in the form of a needle, 0.70 × 0.20 × 0.15 mm, coated with microscope oil, was cooled to –60°. The crystal was not stable at that temp. It turned opaque, but recovered at r.t. Hence, X-ray-diffraction data were collected at r.t. on a Bruker P4 diffractometer. The  $\theta/2\theta$ -scan mode was used with a  $1.4^\circ + 2\theta$  ( $\alpha 1, -\alpha 2$ ) scan width, 13°/min scan speed and  $2\theta_{\max} = 100^\circ$  (1.0 Å resol.). The crystal parameters are C<sub>47</sub>H<sub>82</sub>N<sub>8</sub>O<sub>11</sub> · H<sub>2</sub>O, space group C2,  $a = 34.184(5)$  Å,  $b = 10.673(3)$  Å,  $c = 18.965(4)$  Å,  $\beta = 120.440(10)^\circ$ ,  $V = 5966(2)$  Å<sup>3</sup>, 4 molecules/cell,  $d = 1.061$  mg/m<sup>3</sup>. The number of observed X-ray reflections was rather limited, ca. 35% of the Cu sphere, hence, not sufficient for direct phase determination for solving the structure. The structure was solved by reducing the symmetry of the space group to *P1* and using a fragment based on the known structure of **3** as a model in a vector search procedure. It revealed the orientation of the fragment in the cell of **2**. Subsequently, the correctly placed fragment was used in a phase-expansion procedure with the tangent formula [38], alternating with E-maps to derive the location of the remainder of the atoms. The symmetry elements observed between the two molecules found in this fashion in space group *P1* led to the placement of **2** in space group *C2*. For 1448 reflections observed with  $|F_o| > 4.0\sigma$ , the agreement factor *R1* was 8.9%. The least-squares program used was Siemens SHELXTL, version 5.03 (Iselin, N.J.).

The backbone and side-chain torsion angles and H-bond parameters are summarized in Tables 4 and 5.

## REFERENCES

- [1] L. Pauling, R. B. Corey, H. R. Branson, *Proc. Natl. Acad. Sci. U.S.A.* **1951**, *37*, 205.  
[2] L. Pauling, R. B. Corey, *Proc. Natl. Acad. Sci. U.S.A.* **1951**, *37*, 721.  
[3] G. N. Ramachandan, C. Ramakrishnan, V. Sasisekharan, *J. Mol. Biol.* **1963**, *7*, 95.  
[4] G. N. Ramachandran, C. Ramakrishnan, *Biophys. J.* **1965**, *5*, 909.  
[5] J. S. Richardson, *Adv. Protein Chem.* **1981**, *34*, 164.  
[6] J. Venkatraman, S. C. Shankaramma, P. Balaram, *Chem. Rev.* **2001**, *101*, 313.  
[7] V. J. Hruby, F. Al-Obeidi, W. M. Kazmirski, *Biochem. J.* **1990**, *268*, 249.  
[8] C. Toniolo, *Crit. Rev. Biochem.* **1980**, *9*, 1.  
[9] J. M. Fernandez-Santin, J. Aymami, A. Rodriguez-Galan, S. Munoz-Guerra, J. A. Subirana, *Nature* **1984**, *311*, 53.  
[10] C. Aleman, J. J. Navas, S. Munoz-Guerra, *Biopolymers* **1997**, *41*, 721.  
[11] D. Seebach, M. Overhand, F. N. M. Kuhnle, B. Martinini, L. Oberer, U. Hommel, H. Widmer, *Helv. Chim. Acta* **1996**, *79*, 913.  
[12] D. Seebach, J. L. Matthews, *Chem. Commun.* **1997**, 2011.  
[13] D. Seebach, K. Gademann, J. V. Schreiber, J. L. Matthews, T. Hintermann, D. Jaun, L. Oberer, U. Hommel, H. Widmer, *Helv. Chim. Acta* **1997**, *80*, 2033.  
[14] D. Seebach, A. Abele, K. Gademann, G. Guchard, T. Hintermann, B. Jaun, J. L. Matthews, J. V. Schreiber, L. Oberer, U. Hommel, H. Widmer, *Helv. Chim. Acta* **1998**, *81*, 932.  
[15] D. Seebach, J. V. Schreiber, S. Abele, *Helv. Chim. Acta* **2000**, *83*, 34.  
[16] D. H. Appella, L. A. Christianson, I. L. Karle, D. R. Powell, S. H. Gellman, *J. Am. Chem. Soc.* **1996**, *118*, 13071.  
[17] S. Krauthauser, L. A. Christianson, D. R. Powell, S. H. Gellman, *J. Am. Chem. Soc.* **1997**, *119*, 11719.  
[18] J. J. Barchi, X. L. Huang, D. H. Appella, L. A. Christianson, A. R. Durell, S. H. Gellman, *J. Am. Chem. Soc.* **2000**, *122*, 271.  
[19] R. P. Cheng, S. H. Gellman, W. F. DeGrado, *Chem. Rev.* **2001**, *101*, 3219.  
[20] I. L. Karle, A. Pramanik, A. Banerjee, S. Bhattacharjya, P. Balaram, *J. Am. Chem. Soc.* **1997**, *119*, 9087.  
[21] T. Hintermann, D. Seebach, *Chimia* **1997**, *50*, 244.  
[22] D. Seebach, M. Rueping, P. I. Arvidsson, T. Kimmmerlin, P. Micuch, C. Noti, D. Langenegger, D. Hoyer, *Helv. Chim. Acta* **2001**, *84*, 3503.  
[23] A. Banerjee, P. Balaram, *Curr. Sci.* **1997**, *73*, 1067.  
[24] S. C. Shankaramma, S. K. Singh, A. Sathyamurthy, P. Balaram, *J. Am. Chem. Soc.* **1999**, *121*, 5360.  
[25] D. Seebach, S. Abele, K. Gademann, B. Jaun, *Angew. Chem., Int. Ed.* **1999**, *38*, 1595.  
[26] D. Seebach, S. Abele, T. Sifferlen, M. Hanggi, S. Grunner, P. Seiler, *Helv. Chim. Acta* **1998**, *81*, 2218.  
[27] Y. J. Chung, L. A. Christianson, H. E. Stanger, D. R. Powell, S. H. Gellman, *J. Am. Chem. Soc.* **1998**, *120*, 10555.  
[28] S. K. Awasthi, S. Raghothama, P. Balaram, *Biochem. Biophys. Res. Commun.* **1995**, *216*, 375.  
[29] S. Raghothama, S. K. Awasthi, P. Balaram, *J. Chem. Soc., Perkin Trans. 2* **1998**, 137.  
[30] I. L. Karle, S. K. Awasthi, P. Balaram, *Proc. Natl. Acad. Sci. U.S.A.* **1996**, *93*, 8189.  
[31] I. L. Karle, H. N. Gopi, P. Balaram, *Proc. Natl. Acad. Sci. U.S.A.* **2002**, *99*, 5160.  
[32] C. Zhao, P. L. Polavarapu, C. Das, P. Balaram, *J. Am. Chem. Soc.* **2000**, *122*, 8034.  
[33] I. L. Karle, H. N. Gopi, P. Balaram, *Proc. Natl. Acad. Sci. U.S.A.* **2001**, *98*, 3716.  
[34] B. L. Sibanda, T. L. Blundell, J. M. Thornton, *J. Mol. Biol.* **1989**, *206*, 759.  
[35] K. Pluncinska, B. Liberek, *Tetrahedron* **1987**, *43*, 3509.  
[36] C. Guibourdenche, D. Seebach, *Helv. Chim. Acta* **1997**, *80*, 1.  
[37] M. Bodanszky, A. Bodanszky, 'The Practice of Peptide Synthesis', Springer, Berlin, 1984, p. 138.  
[38] J. Karle, *Acta Crystallogr., Sect. B* **1968**, *24*, 182.

Received June 13, 2002